Mon. Not. R. Astron. Soc. **000**, 000–000 (0000) Printed 27 January 2009 (MN LATEX style file v2.2)

Diverging UV and Hα fluxes of star forming galaxies predicted by the IGIMF theory

Jan Pflamm-Altenburg[1⋆], Carsten Weidner[2⋆] and Pavel Kroupa[1⋆]
[1] *Argelander-Institut für Astronomie, Universität Bonn, Auf dem Hügel 71, D-53121 Bonn, Germany*
[2] *Scottish Universities Physics Alliance (SUPA), School of Physics and Astronomy, University of St. Andrews, North Haugh, St. Andrews, Fife KY16 9SS, UK*

arXiv:0901.4335v1 [astro-ph.GA] 27 Jan 2009

accepted 19 January 2009 - The definitive version is available at www.blackwell-synergy.com.

ABSTRACT
Although the stellar initial mass function (IMF) has only been directly determined in star clusters it has been manifoldly applied on galaxy-wide scales. But taking the clustered nature of star formation into account the galaxy-wide IMF is constructed by adding all IMFs of all young star clusters leading to an integrated galactic initial mass function (IGIMF). The IGIMF is top-light compared to the canonical IMF in star clusters and steepens with decreasing total star formation rate (SFR). This discrepancy is marginal for large disk galaxies but becomes significant for SMC-type galaxies and less massive ones. We here construct IGIMF-based relations between the total FUV and NUV luminosities of galaxies and the underlying SFR. We make the prediction that the Hα luminosity of star forming dwarf galaxies decreases faster with decreasing SFR than the UV luminosity. This turn-down of the Hα-UV flux ratio should be evident below total SFRs of 10^{-2} $M_\odot$ yr^{-1}.

Key words: cosmology: observations — galaxies: evolution — galaxies: fundamental parameters — galaxies: irregular, disk — stars: luminosity function, mass function — stars: formation

1 INTRODUCTION

In order to determine the current star formation rate (SFR) of galaxies certain regions of the electromagnetic spectrum have to be measured which have contributions mainly by young stars. For example, the Hα emission line has its origin in the recombination of ionised hydrogen and its intensity is a measure for the amount of currently existing short-lived massive stars. On the other hand, UV luminosities allow a more direct access to the young stellar population.

Altough the mass spectrum of UV-luminosity contributing stars extends to much lower limits than for the Hα luminosity only a massive-star formation rate is measured. In order to estimate the total galaxy-wide star formation rate an extrapolation to the low-mass spectrum of newly formed stars has to be done. This extrapolation is normally based on the galaxy-wide application of a universal stellar initial mass function (IMF) leading to linear relations between the total Hα and UV luminosity and the underlying total SFR (Kennicutt 1983; Kennicutt et al. 1994; Kennicutt 1998).

While the IMF seems to be universal (Kroupa 2001, 2002) its form has only been determined directly on star cluster scales. The canonical IMF, $\xi(m)$, is a two-part power-law in the stellar regime, $dN = \xi(m)\, dm$ being the number of stars in the infinitesimal mass range from m to $m+dm$ and $\xi(m) \propto m^{-\alpha_i}$, $\alpha_1 = 1.3$ for $0.1 \leq m/M_\odot < 0.5$, $\alpha_2 = 2.35$ for $0.5 \leq m/M_\odot \leq m_{\rm max}$, where $m_{\rm max}$ is the maximal stellar mass in a star cluster with the embedded (i.e. birth) stellar mass $M_{\rm ecl}$.

This canonical IMF (or a similar one, e.g. Chabrier 2003) has traditionally been applied on galaxy-wide scales. But most stars form in star clusters (Tutukov 1978; Lada & Lada 2003). Thus the galaxy-wide IMF has to be constructed by adding all young stars of all young star clusters (Kroupa & Weidner 2003; Weidner & Kroupa 2006). This integrated galactic initial mass function (IGIMF) is steeper than the canonical IMF in star clusters and steepens with decreasing total SFR (Weidner & Kroupa 2005; Pflamm-Altenburg, Weidner & Kroupa 2007) due to the combination of two effects: i) The most massive star, $m_{\rm max}$, in a star cluster is a function of the total stellar mass of the young embedded star cluster, $M_{\rm ecl}$, (Weidner & Kroupa 2006), and ii) the most massive young embedded star cluster, $M_{\rm ecl,max}$, is a function of the total SFR of a galaxy (Weidner, Kroupa & Larsen 2004). Similar to the IMF in star clusters the embedded cluster mass function (ECMF), which describes the mass spectrum of newly formed star

⋆ email: jpflamm@astro.uni-bonn.de, cw60@st-andrews.ac.uk, pavel@astro.uni-bonn.de

clusters, follows a power-law distribution function in galaxies (Lada & Lada 2003; Weidner et al. 2004; Bastian 2008). Due to the $M_{\rm ecl,max}$-SFR relation the number and total mass ratio of high-mass and low-mass young embedded star clusters decreases with decreasing SFR. Because of the $m_{\rm max}$-$M_{\rm ecl}$ relation massive stars are predominantly formed in high-mass clusters, so the number and mass fraction of massive stars among all galaxy-wide newly formed stars decreases with decreasing SFR, too. Therefore the IGIMF becomes steeper with decreasing SFR and, consequently, the fundamental prediction by the IGIMF-theory is that integrated properties which are sensitive to the presence of massive stars decrease faster with decreasing SFR than the SFR! We call this basic phenomenon the IGIMF-effect.

Recently observational evidence has become available that the galaxy-wide IMF seems to be steeper than the universal IMF in star clusters: The Milky Way disk IMF index $\alpha_3 \approx 2.7$ (for $m \geq 1\ M_\odot$) is larger than the canonical Salpeter IMF index of $\alpha_3 \approx 2.35$ (Kroupa et al. 1993). Using the Scalo index, i.e. $\alpha_3 = 2.7$, Diehl et al. (2006) find a consistency between the supernova rate as derived from the Galactic ^{26}Al gamma-ray flux and that deduced from a survey of local O and B stars, extrapolated to the whole Galaxy (McKee & Williams 1997). Unfortunately, a detailed analysis to which order a galaxy-wide high-mass IMF slope shallower than Scalo can be ruled out is not presented in Diehl et al. (2006).

Additionally, Lee et al. (2004) find that low surface brightness galaxies have much steeper massive-star IMFs than Milky Way-type galaxies. Hoversten & Glazebrook (2008) derived a non-universal stellar IMF in SDSS galaxies based on integrated photometric properties. Bright galaxies have a high-mass slope of ≈ 2.4, whereas fainter galaxies prefer steeper IMFs. Also, galaxies with a lower SFR have a steeper IMF than those with a higher SFR therewith confirming the basic prediction of the IGIMF theory (Weidner & Kroupa 2005). Based on HST-star counts in the SMC-type galaxy NGC 4214 Úbeda et al. (2007) derived a massive-star IMF slope of 2.8, being steeper than the Salpeter value. Vanbeveren (1983) had already pointed out that a steepening of a field IMF compared to the IMF in associations may be expected.

Interestingly, these steeper galaxy-wide IMFs appear to be in contradiction to cosmic IMF studies where the cosmic stellar mass density is compared with the integrated cosmic star formation rate history. Wilkins et al. (2008) finds that only a high-mass IMF slope of about 2.15 will put both cosmic constrains into agreement in the low-redshift universe. However, their method is an indirect one and depends on many other parameters.

In contrast, the Scalo (1986) high-mass IMF slope of $\alpha_3 = 2.7$ implemented by Kroupa et al. (1993) in their adoption of the standard Galactic-field IMF is based on star counts determining the present-day mass function (PDMF) converted into an IMF. A steeper than Salpeter high-mass field IMF slope of the Milky Way is also found by Reid, Gizis & Hawley (2002) who obtained a slope of 2.5–2.8 at high masses. The conversion of the PDMF into an IMF requires the assumption of a certain star formation history. In Reid et al. (2002) a constant star formation rate is assumed based on the study by Gizis, Reid & Hawley (2002). But Elmegreen & Scalo (2006) demonstrate that true variations in the star formation rate over times from $\sim 2\times10^6$ to 10^9 yr can produce variations in the PDMF slope leading to a wrong conclusion of a varying IMF slope if the star formation history is assumed incorrectly to vary more smoothly or not at all. Thus the assumption of a constant star formation rate in Reid et al. (2002) may break down on time-scales shorter than 10^8 yr. The Scalo IMF index, $\alpha_3 = 2.7$, is based on an exponentionally changing star formation rate with a time constant of 9 to 15 Gyr. A varying time constant between 9 and 15 Gyr does not influence the derived index significantly. However, short time-scale fluctuations as considered by Elmegreen & Scalo (2006) are not included in the analysis by Kroupa et al. (1993). Up to what mass the IMFs derived from the PDMFs in Kroupa et al. (1993) and Reid et al. (2002) are reliable is an open question, and the local field IMF inferred from the PDMF therefore needs further detailed studies.

Additionally, galaxy evolution models with a steeper than Salpeter high-mass IMF slope are in agreement with observed chemical properties of the solar vicinity (Romano et al. 2005) and the low mass-to-light ratios of disk galaxies inferred from dynamical arguments (Portinari et al. 2004). In this view it might be doubtful that the steeper than Salpter Milky Way field IMFs by Kroupa et al. (1993) and Reid et al. (2002) obtained from PDMF star counts are only due to star formation rate variations as a galaxy-wide long-term Salpeter high mass IMF index would leed to expected present day chemical properties of the solar vicinity which might be in conflict with local observations.

Chemical evolution models of galaxies (Köppen, Weidner & Kroupa 2007) have recently shown that the IGIMF-theory directly leads to a mass-metallicity relation of galaxies as observed (Tremonti et al. 2004). Additionally, the alpha-element abundances in the IGIMF theory vary with the mass of early-type galaxies as is observed (Recchi et al. 2009). Furthermore, the Hα luminosity of a galaxy is related to the presence of short-lived massive stars such that the total Hα-luminosity of a galaxy scales non-linearly with the total SFR (Pflamm-Altenburg et al. 2007). Consequently, the SFRs as deduced from Hα luminosities of dwarf irregular galaxies are significantly underestimated. Applying the IGIMF based $L_{\rm H\alpha}$-SFR relation to a large sample of star forming galaxies leads to a linear star formation law for gas rich galaxies, $SFR \propto M_{\rm HI}$, without any fine-tuning or parameter adjustment, where $M_{\rm HI}$ is the mass of neutral gas. It follows that star forming galaxies have the same constant gas depletion time scale of about 2.9 Gyr independently of the galaxy gas mass (Pflamm-Altenburg and Kroupa, submitted).

The IGIMF-effect should be more pronounced for integrated properties which are more sensitive to the most massive stars. Contrary to the Hα luminosity which depends on the presence of ionizing massive stars ($\gtrsim 10 M_\odot$), UV luminosities have their main contribution from long-lived B stars. Therefore, it is expected that the UV-SFR relation is much less SFR- and IGIMF-dependent than the Hα-SFR relation.

Indeed, observations of large disk galaxies in the UV-band by GALEX revealed star formation beyond the Hα cutoff in the very outer disks of galaxies where the surface gas density is much lower than the hitherto assumed existing star formation threshold surface density. This poses

a challenge to current understanding (Boissier et al. 2007). This fundamental discrepancy is solved naturally in the context of the IGIMF-theory. As the IGIMF-theory describes the galaxy-wide IMF its local analogon, the local integrated galactic initial mass function (LIGIMF), is required to address the problem of differing Hα and UV star formation rate surface densities. This has been be achieved straightforwardly by replacing all galaxy-wide quantities in the IGIMF-theory by their corresponding surface densities (Pflamm-Altenburg & Kroupa 2008). The LIGIMF-theory perfectly reproduces the observed relation between the local Hα luminosity surface density and the local gas mass surface density and the radial Hα cut-off in disk galaxies. A basic assumption was that the UV-luminosity shows no IGIMF-effect and scales linearly with the SFR. A definite proof for this ansatz was not given but is presented here.

We first describe how the IGIMF based UV-SFR relation is calculated (Sec. 2), present the relation (Sec. 3) and confirm the validity of the ansatz made in Pflamm-Altenburg & Kroupa (2008). Finally, we calculate the expected variation of the Hα-UV luminosity ratio with decreasing total SFR (Sec.4).

2 CODE

In order to compute the NUV and FUV luminosities of galaxies for a given SFR we use the second release of the spectral evolution code PEGASE by Fioc & Rocca-Volmerange (1997, 1999). The filter-curves of the GALEX-FUV and NUV passbands have been obtained from the GALEX webpage. The number of points of the tabulated transmission curves has been reduced to get a simpler description of the filter curves (Table 2). The filter-curves are then internally calibrated by PEGASE to the AB system (Oke 1974). All magnitudes in this paper are absolute AB magnitiudes unless stated otherwise. An AB-magnitude is related to a monochromatic flux density, f_ν in erg s^{-1} cm^{-2} Hz^{-1}, by

$$m_{\rm AB} = -2.5\ \log_{10} f_\nu - 48.60 \qquad (1)$$

given in Oke (1974)[1]. An absolute AB-magnitude can then be converted into a monochromatic luminosity, L_ν in erg s^{-1} Hz^{-1}, by

$$L_\nu = 10^{-0.4(M_{\rm AB}-51.60)}\ . \qquad (2)$$

The IGIMFs are calculated for different SFRs using equation 11 of Pflamm-Altenburg et al. (2007). The underlying IMF in star clusters has the canonical form. The observed physical upper mass limit for stars of about 150 $M_\odot$ (Weidner & Kroupa 2004; Figer 2005; Oey & Clarke 2005; Koen 2006; Maíz Apellániz et al. 2007) has been reduced to $m_{\rm max*} = 120 M_\odot$ because the stellar evolution models included in PEGASE only cover the mass range from 0.1 to 120 $M_\odot$. This lower physical upper mass limit does not lead to any falsification of the expected IGIMF-UV luminosities as shown in Sec. 3.

We choose an embedded cluster mass function (ECMF) which is a single-part power law with a Salpeter index $\beta_1 = 2.35$ between 5 $M_\odot$ and $M_{\rm ecl,max}(SFR)$, where $M_{\rm ecl,max}(SFR)$ is the upper mass limit of the ECMF which is a function of the total SFR (Weidner et al. 2004). An ECMF with slope 2.35 best reproduces the observed relation between the infrared SFRs of galaxies and their most massive young star cluster (Weidner et al. 2004). Therefore, the IGIMF model with a Salpter-slope ECMF is the so-called standard model (Weidner & Kroupa 2005). This slope is steeper than the ECMF slope of 2 observed for embedded low-mass clusters in the solar neighbourhood (Lada & Lada 2003). A shallower ECMF slope has a higher ratio of high-mass star clusters to low-mass star clusters and thus leads to a smaller IGIMF effect than an IGIMF model with a steeper ECMF slope. In order to explore the full range of possible IGIMF effects we also use a two-part power law with $\beta_1 = 1.0$ between 5 $M_\odot$ and 50 $M_\odot$ and $\beta_2 = 2.0$ between 50 $M_\odot$ and $M_{\rm ecl,max}(SFR)$ for the ECMF to minimise the IGIMF effect. This is the so-called minimal1-IGIMF (Pflamm-Altenburg et al. 2007, table 1 therein).

The resultant IGIMFs have been fitted by multi-part power laws[2] and included into PEGASE.

Table 1. GALEX-filter fits.

λ	$T_{\rm NUV}(\lambda)$	λ	$T_{\rm FUV}(\lambda)$
1690	0.000	1340	0.000
1700	0.025	1352	0.121
1750	0.033	1370	0.177
1819	0.130	1380	0.178
1858	0.191	1400	0.122
1904	0.272	1427	0.257
1951	0.336	1450	0.342
2001	0.450	1470	0.367
2050	0.471	1480	0.368
2103	0.530	1500	0.349
2150	0.595	1520	0.347
2200	0.617	1530	0.329
2248	0.566	1550	0.262
2303	0.527	1610	0.256
2350	0.477	1651	0.159
2405	0.510	1698	0.124
2450	0.535	1750	0.106
2556	0.514	1799	0.012
2599	0.501	1810	0.000
2650	0.457		
2700	0.376		
2801	0.107		
2850	0.035		
2900	0.013		
2947	0.014		
3000	0.019		
3010	0.000		

The tabulated transmission curves are obtained from the GALEX-webpage and are piecewisely fitted in order to reduce the number of segments. The transmission curves $T(\lambda)$ of the NUV and FUV passbands at the wavelength λ in Å correspond to the number fraction of photons transmitted.

[1] Note that there are typos in younger papers (Oke & Gunn 1983; Oke 1990, e.g.).

[2] The data files of the fits and an IGIMF-calculation/fit tool are available as downloads at `www.astro.uni-bonn.de`

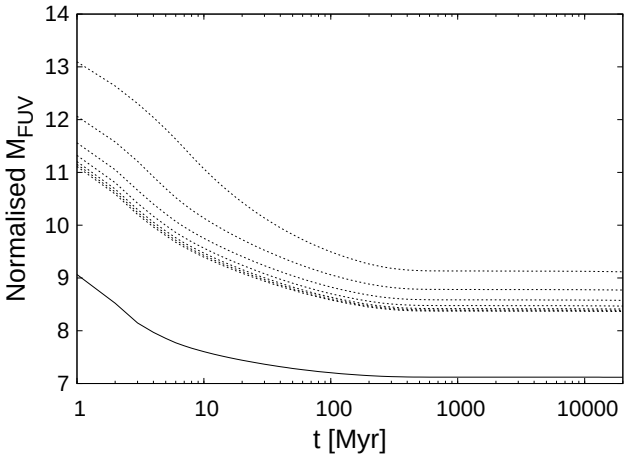

Figure 1. Evolution of the normalised FUV-magnitude, $M_{\rm FUV,norm}$, for a constant SFR and a constant metallicity ($Z = 0.02$). The solid curve refers to the canonical IMF. The dotted curves refer to the standard IGIMF corresponding to different total SFRs. From bottom to top: 10^3, 10^2, 10, 1, 10^{-1}, 10^{-2}, and 10^{-3} $M_\odot$ yr^{-1}.

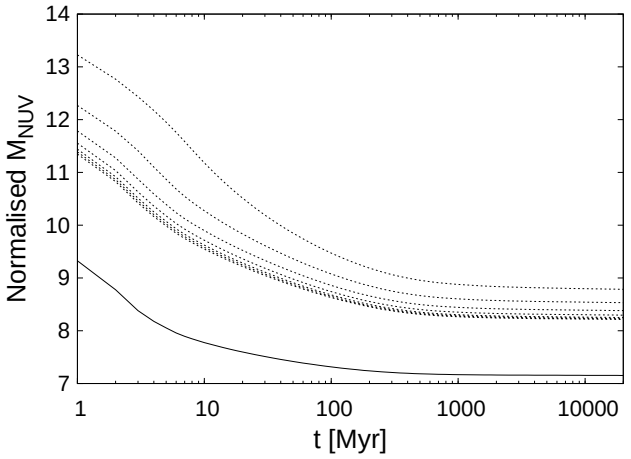

Figure 2. Same as Fig. 1, but for NUV.

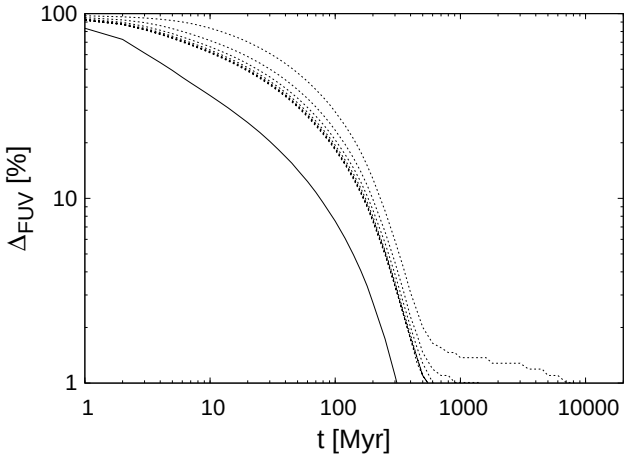

Figure 3. Evolution of the relative FUV-luminosity difference, $\Delta_{\rm FUV}$, compared to the equilibrium luminosity, $L_{\rm e}$, at 20 Gyr. The normalised FUV luminosity, $L_{\rm t}$, at the time t from Fig. 1 corresponds to the normalised FUV magnitude, $m_{\rm t}$, by $\frac{L_{\rm t}}{L_{\rm e}} = 10^{-0.4(m_{\rm t}-m_{\rm e})}$. The plotted value is then calculated by equation 5. Note that the value of $\Delta_{\rm FUV}$ does not depend on the normalisation constant.

3 UV-SFR RELATION

The modified PEGASE code with the new filters and the IGIMF has been run with its default values to create a grid of galaxy evolution models. Each model has a constant-SFR scenario and no evolution of the stellar metallicity. The output by PEGASE is normalised by the total mass, $M_{\rm tot}$, where $M_{\rm tot} = M_{\rm stars} + M_{\rm gas}$. The PEGASE calculations start at $t = 0$ with $M_{\rm gas} = M_{\rm tot}$ and $M_{\rm stars} = 0$ and stop at $t = 20$ Gyr when $M_{\rm tot} = \int_0^{20\ {\rm Gyr}} SFR\ dt = SFR \times 20$ Gyr such that $M_{\rm tot}$=const throughout the integrations. The absolute FUV and NUV magnitudes, $M_{\rm UV}$, and the SFR are obtained from their normalised values by

$$M_{UV} = M_{\rm UV,norm} - 2.5 \log_{10} M_{\rm tot} \ , \qquad (3)$$

and

$$SFR = SFR_{\rm norm}\ M_{\rm tot} \ . \qquad (4)$$

A relation between the absolute UV magnitude and the SFR can be easily obtained by combining these two equations and removing the normalisation factor/constant. The normalised UV magnitudes evolve with time and settle into an equilibrium magnitude (Fig. 1 and 2). At each time the normalised FUV magnitude is fainter for a lower normalised SFR as the IGIMF becomes steeper with decreasing SFR, i.e. the fraction of FUV contributing stars becomes smaller with decreasing SFR.

How fast the UV-magnitude-t curves converge against their equilibrium value (evaluated at $t = 20$ Gyr) can be seen in Fig. 3 and 4. The normalised UV magnitudes have been converted into a normalised luminosity and the relative deviation,

$$\Delta_{\rm FUV} = \frac{L(t) - L_{\rm e}}{L_{\rm e}} = \frac{L(t)}{L_{\rm e}} - 1 \ , \qquad (5)$$

of the luminosity, $L(t)$, at the time t from the equilibrium luminosity, $L_{\rm e}$, at $t = 20$ Gyr has been plotted as a function of the time. The value of $\Delta_{\rm FUV}$ does not depend on the normalisation constant in equation 3 as the normalisition constant, $M_{\rm tot}$, in equation 3 corresponds to a normalisation factor in equation 4 which cancels out. All FUV-IGIMF models differ by less than 2 per cent from the equilibrium value after 400 Myr, whereas the NUV-IGIMF model are closer than 10 per cent to the equilibrium value after 1 Gyr. Thus, using the FUV magnitude can only lead to SFR estimations averaged over ≈ 400 Myr. Both passbands approach the equilibrium value more slowly for lower SFRs. With decreasing SFR the standard IGIMF becomes steeper and the upper mass limit reduces. Thus the mean life-time of UV contributing stars increases and the system takes longer to approach the equilibrium state.

The resulting FUV/NUV-SFR relations are shown in Fig. 5 and 6 for two IGIMF-models, standard and minimal1, and the classical linear case, where the IGIMF is identical to the canonical IMF. Both IGIMF models are fitted by a polynomial of fourth order,

$$y = a_0 + a_1 x + a_2 x^2 + a_3 x^3 + a_4 x^4 \ , \qquad (6)$$

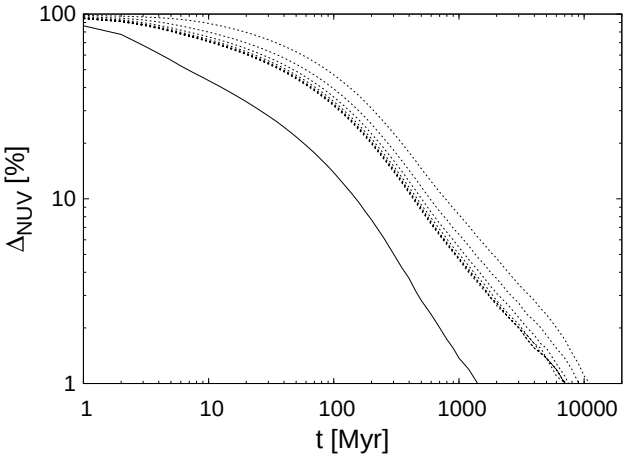

Figure 4. Same as Fig. 3, but for $\Delta_{\rm NUV}$.

Table 3. UV-SFR fit (IMF).

filter	Z	μ
FUV	0.0001	-4.01
FUV	0.0004	-3.95
FUV	0.004	-3.83
FUV	0.008	-3.75
FUV	0.02	-3.63
FUV	0.05	-3.46
NUV	0.0004	-3.91
NUV	0.004	-3.75
NUV	0.008	-3.68
NUV	0.02	-3.60
NUV	0.05	-3.49

The SFR-UV-magnitude relations for a galaxy-wide canonical IMF for different metallicities Z is expressed by Eq. 9.

with

$$x = M_{\rm UV}\ [\text{AB mag}] \tag{7}$$

and

$$y = \log_{10} \frac{SFR}{M_\odot\ \text{yr}^{-1}}\ . \tag{8}$$

The resulting co-efficients are listed in Table 2 for different metallicities Z. The UV-SFR relation for the unchanging canonical IMF model can be expressed by

$$\frac{SFR}{M_\odot\ \text{yr}^{-1}} = 10^{-0.4(M_{\rm UV}-\mu)-6} \tag{9}$$

and Table 3. By combining equations 2 and 9 a relation between the monochromatic luminosity, L_ν in erg s^{-1} Hz^{-1}, and the SFR in $M_\odot$ yr^{-1} can be obtained for the case of a simple galaxy-wide IMF,

$$SFR/L_\nu = 10^{0.4\mu-26.64}\ . \tag{10}$$

For $Z = 0.02$ the ratio becomes

$$SFR/L_\nu = 8.09 \times 10^{-29}\ , \tag{11}$$

which is only a factor 1.3 less than the factor given in Salim et al. (2007) and a factor 1.7 less than in Kennicutt (1998). These small differences are expected as different

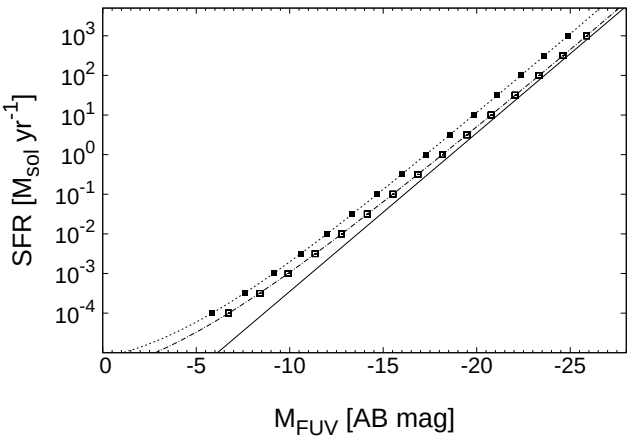

Figure 5. The underlying total SFR as a function of the equilibrium absolute FUV-magnitude for a constant metallicity ($Z = 0.02$) and two IGIMF models, standard (black squares) and minimal1 (open squares), and the canonical IMF (solid line). The two dotted curves represent polynomial fits (equations 6–8 and Table 2) to the IGIMF models. The canonical IMF model can be described by equation 9 and Table 3.

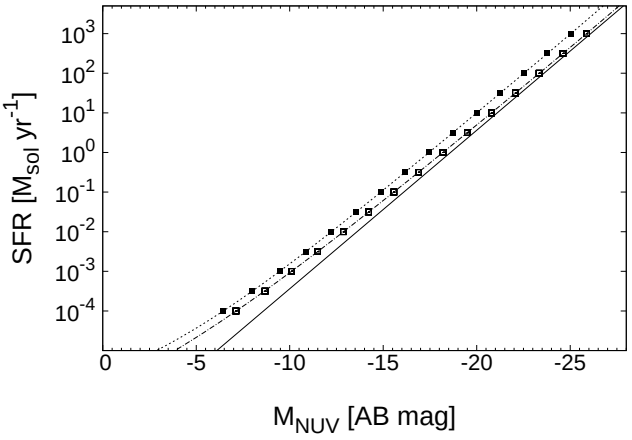

Figure 6. Same as Fig. 5, but for NUV.

stellar population models, different methods to define a UV-SFR relation, different metallicity considerations, and slightly different passbands are used.

Keeping the metallicity constant is justified for calculating the equilibrium UV magnitude for a given SFR as the equilibrium is achieved within ≈ 400 Myr and the metallicity of a galaxy is not expected to change significantly within this period. But the absolute constant metallicity may depend on the given SFR because galaxies with lower SFRs are also typically less massive and have lower total metallicities than typical galaxies with high SFRs. The standard-IGIMF-SFR is plotted as a function of the equilibrium FUV-magnitude for different metallicities in Fig. 7. A very metal poor galaxy ($Z = 0.0001$) has roughly the same FUV-magnitude as a metal rich galaxy ($Z = 0.05$) with a 0.5 dex higher SFR. In particular, applying the FUV-SFR relation for $Z = 0.02$ (Milky Way-type galaxies) on a SMC-type dwarf galaxy with $Z \approx 0.004$ would result in a SFR which is approximately 0.2 dex too high. Such differences are well within any ob-

Table 2. UV-SFR fit (IGIMF).

model	filter	Z	a_0	a_1	a_2	a_3	a_4
std-IGIMF	FUV	0.0001	-6.25	-0.234	0.0105	0.000311	3.57e-06
std-IGIMF	FUV	0.0004	-6.07	-0.216	0.0116	0.000345	3.95e-06
std-IGIMF	FUV	0.004	-5.60	-0.151	0.0165	0.000509	6.08e-06
std-IGIMF	FUV	0.008	-5.38	-0.121	0.0187	0.000585	7.08e-06
std-IGIMF	FUV	0.02	-5.11	-0.0870	0.0214	0.000683	8.43e-06
std-IGIMF	FUV	0.05	-4.94	-0.0705	0.0227	0.000729	9.07e-06
min1-IGIMF	FUV	0.0001	-6.54	-0.270	0.00734	0.000210	2.45e-06
min1-IGIMF	FUV	0.0004	-6.38	-0.254	0.00806	0.000226	2.59e-06
min1-IGIMF	FUV	0.004	-5.98	-0.197	0.0120	0.000353	4.18e-06
min1-IGIMF	FUV	0.008	-5.74	-0.162	0.0145	0.000438	5.27e-06
min1-IGIMF	FUV	0.02	-5.47	-0.124	0.0173	0.000533	6.52e-06
min1-IGIMF	FUV	0.05	-5.28	-0.103	0.0187	0.000577	7.03e-06
std-IGIMF	NUV	0.0001	-6.90	-0.325	0.00444	0.000124	1.34e-06
std-IGIMF	NUV	0.0004	-6.75	-0.312	0.00519	0.000144	1.55e-06
std-IGIMF	NUV	0.004	-6.23	-0.251	0.00931	0.000273	3.11e-06
std-IGIMF	NUV	0.008	-5.94	-0.211	0.0122	0.000368	4.33e-06
std-IGIMF	NUV	0.02	-5.58	-0.163	0.0158	0.000494	5.98e-06
std-IGIMF	NUV	0.05	-5.30	-0.125	0.0186	0.000590	7.22e-06
min1-IGIMF	NUV	0.0001	-7.13	-0.362	0.00127	2.08e-05	1.72e-07
min1-IGIMF	NUV	0.0004	-7.00	-0.353	0.00152	2.04e-05	9.75e-08
min1-IGIMF	NUV	0.004	-6.55	-0.298	0.00502	0.000128	1.39e-06
min1-IGIMF	NUV	0.008	-6.27	-0.254	0.00817	0.000233	2.74e-06
min1-IGIMF	NUV	0.02	-5.96	-0.209	0.0112	0.000333	4.02e-06
min1-IGIMF	NUV	0.05	-5.66	-0.163	0.0145	0.000438	5.28e-06

The SFR-absolute-UV-magnitude relations are fitted by a polynomal of fourth order according to Eq. 6–8 for two IGIMF models, standard and minimal1, and different metallicities Z.

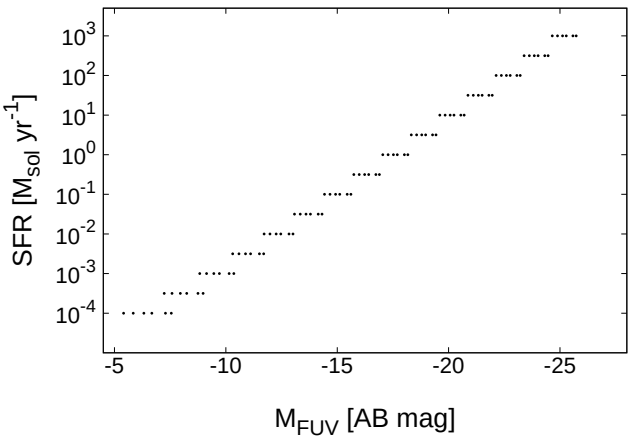

Figure 7. The SFR as a function of the equilibrium FUV-magnitude for different metallicities (black squares from right to left: Z = 0.0001, 0.0004, 0.004, 0.008, 0.02 and 0.05).

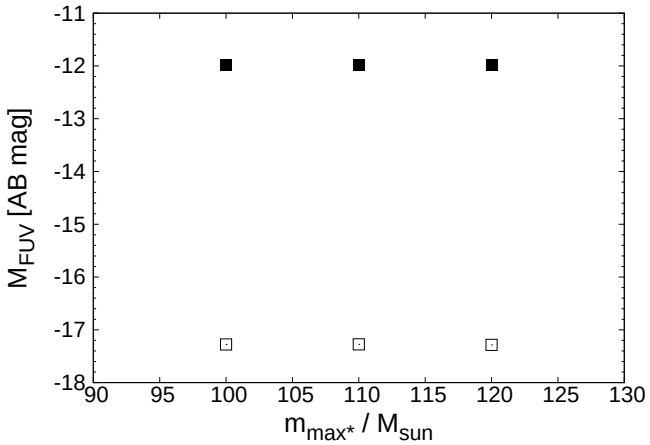

Figure 8. The equilibrium FUV-magnitude as a function of the physical upper mass limit, $m_{\rm max*}$, for a constant metallicity (Z = 0.02) and two different SFRs of 10^{-2} (black squares) and 1 $M_\odot$ yr^{-1} (open squares) for the case of the standard IGIMF.

servational uncertainties and metallicity differences can be ignored for the present.

A second parameter dependence of the UV-SFR relation may be due to the choice of the physical stellar upper mass limit, $m_{\rm max*}$. We here chose $m_{\rm max*}$ = 120 M$_\odot$ as the stellar evolution models included in PEGASE do not allow a higher mass limit. But the true upper mass limit may lie at about 150 $M_\odot$ (Weidner & Kroupa 2004; Figer 2005; Oey & Clarke 2005; Koen 2006; Maíz Apellániz et al. 2007). To test for a possible physical upper-mass-limit dependence we calculate the FUV equilibrium magnitude for the standard IGIMF and a constant metallicity of Z = 0.02 but with $m_{\rm max*}$=100, 110 and 120 $M_\odot$. As can be seen in Fig. 8 there is no influence on the FUV magnitude when varying the physical stellar upper mass limit above 100 $M_\odot$. Because the NUV magnitude is less sensitive to the presence of high-mass stars than FUV the non-dependence on the physical upper mass limit holds for NUV, too.

4 COMPARING THE UV– AND Hα–SFR

As already mentioned the UV-SFR relation is expected to be very much less sensitive to the IGIMF effect and thus much closer to linearity than the corresponding Hα-SFR relation. In order to demonstrate this we predict the result a classical observer would get when comparing UV and Hα based SFRs obtained with a linear luminosity-SFR relation.

For a given true total SFR the Hα luminosity and the total FUV magnitude are calculated for the IGIMF theory. The FUV magnitude is calculated using the FUV-SFR relation constructed in Section 3. Although the PEGASE output provides Hα luminosities, the Hα-SFR relation from Pflamm-Altenburg et al. (2007) is used instead. PEGASE does not include stellar evolution models for stars more massive than 120 $M_\odot$. But the physical stellar upper mass limit is thought to lie around 150 $M_\odot$ (Weidner & Kroupa 2004; Figer 2005; Oey & Clarke 2005; Koen 2006; Maíz Apellániz et al. 2007) which is taken into account in the Hα-SFR relation in Pflamm-Altenburg et al. (2007). As shown in the previous section the exact value of the physical upper mass limit does not have a noticeable influence on the FUV-SFR relation. Contrary, the Hα-SFR relation does appreciably depend on the physical stellar upper mass limit as discussed below. The Hα luminosity is then reconverted into a SFR using the classical linear Hα-SFR relation (Kennicutt et al. 1994; Kennicutt 1998). The IGIMF FUV-magnitude is reconverted into a SFR using the linear relation described by equation 9 based on the invariant canonical IMF.

Both, the theoretical Hα- and the theoretical FUV-luminosity refer to produced radiation, i.e. extinction is not taken into account. The reason is that both produced luminosities and therefore their ratio is only a function of the total SFR. The apparent luminosities and luminosity ratios indeed depend on different extinction effects, thus do not depend on the total SFR but e.g. on the dust content of the target galaxy, the inclination of the target galaxy, and the Galactic latitude and longitude. Thus two galaxies with identical SFRs and produced Hα- and FUV-luminosities can have different observed luminosities. The correction for Galactic and internal extinction has to be done individually for each observed target galaxy.

Fig. 9 shows the expected ratio of the total Hα and FUV luminosity as a function of the total Hα luminosity for two different IGIMF models, standard (open squares) and minimal1 (filled squares), and a constant metallicity ($Z = 0.02$).

Fig. 10 shows the expected UV-Hα SFR-ratio as a function of the true underlying SFR for a constant metallicity ($Z = 0.02$). The ratio is plotted for two IGIMF models, standard (open symbols) and minimal1 (filled symbols), and two different linear Hα-SFR relations, the invariant canonical-IMF based relation from Pflamm-Altenburg et al. (2007) (squares) and the widely used Salpeter-IMF based relation from Kennicutt et al. (1994) (circles).

Below a total SFR of about 10^{-2} $M_\odot$ yr^{-1} the SFR based on Hα flux and an invariant IMF should start to dramatically decrease faster than the SFR based on UV flux and an invariant IMF.

IGIMF model details such as different slopes of the ECMF have only a minor effect on the position and the strength of the Hα-UV turn-down. Furthermore, at first sight it is expected that the classical Hα-SFR should be always lower than the classical UV-SFR: Consider a galaxy which populates its young stellar content according to the IGIMF scenario. The number of O and B stars in this galaxy is smaller than expected if the galaxy-wide IMF were identical to the canonical IMF for the same SFR. In order to get the same total UV and Hα flux for an assumed galaxy-wide invariant IMF the calculated SFR has to be smaller than the true SFR. As the Hα flux decreases faster than the UV flux with decreasing SFR the SFR based on Hα flux and an invariant IMF is always smaller than the SFR based on UV flux and an invariant IMF.

But as shown in the previous section, varying the physical stellar upper mass limit has no influence on the FUV magnitude. On the other hand, the situation is different for

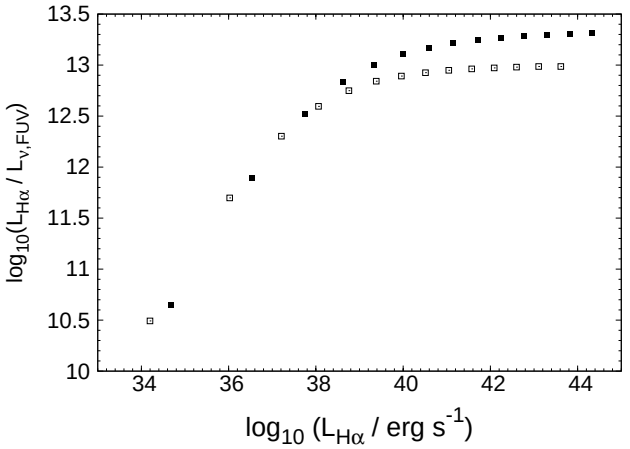

Figure 9. The expected Hα-/UV-luminosity ratio as a function of the Hα luminosity for two different underlying IGIMF models, standard (open squares) and minimal1 (filled squares).

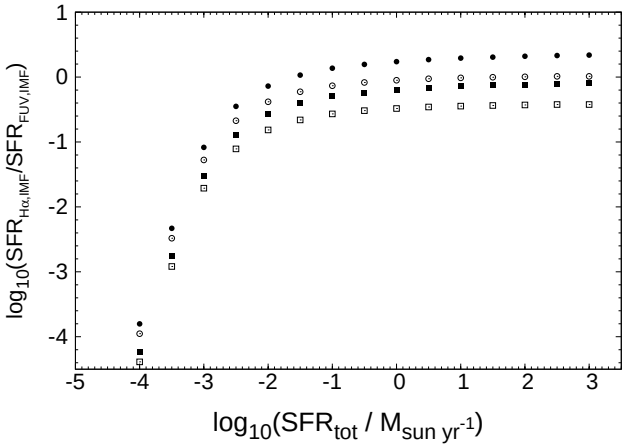

Figure 10. The expected Hα-SFR/UV-SFR ratio when the luminosities are converted into SFRs using classical linear relations for two different underlying IGIMF models, standard (open symbols) and minimal1 (filled symbols), and two different linear Hα-SFR relations, the canonical-IMF based relation from Pflamm-Altenburg et al. (2007) (squares) and the widely used Salpeter-IMF based relation from Kennicutt et al. (1994) (circles).

the Hα luminosity as it depends significantly on the number of very massive stars. The IGIMF model includes an IMF which can be populated up to a physical stellar upper mass limit of 150 $M_\odot$ in agreement with recent observations (Weidner & Kroupa 2004; Figer 2005; Oey & Clarke 2005; Koen 2006; Maíz Apellániz et al. 2007). When using the linear Hα-SFR relation based on the canonical IMF with a physical stellar upper mass limit of 150 $M_\odot$ from Pflamm-Altenburg et al. (2007) the Hα-SFR/UV-SFR ratio converges as expected against unity with increasing SFR. But when calculating the Hα based SFR with the widely used Salpeter-IMF based relation by Kennicutt et al. (1994), which has an upper mass limit of 100 $M_\odot$, the classical Hα based SFRs can be higher than the UV-based SFRs, because the Hα contribution of stars more massive than 100 $M_\odot$ has to be balanced by an artificial higher SFR when taking only stars less massive than 100 $M_\odot$ into account.

5 CONCLUSIONS

Based on the IGIMF theory, which takes the clustered nature of star formation into account, we have constructed a relation between the UV-luminosity of a galaxy and the underlying SFR. In agreement with previous assumptions and expectations we confirm that the UV luminosities of galaxies are much less sensitive to the IGIMF effect than the Hα luminosity. Furthermore, the definite prediction by the IGIMF theory is that around a total SFR of about 10^{-2} $M_\odot$ yr^{-1} the classical IMF based Hα SFR should start to decrease faster than the classical IMF based UV SFR. The position and the strength of the turn-down is nearly IGIMF-model independent. This prediction can be tested by UV-observations of dwarf irregular galaxies with total SFRs in the range of 10^{-4}–10^{-2} $M_\odot$.

We would like to thank Samuel Boissier for helpful comments on this paper. J. P-A. acknowledegs partial support through DFG grant KR1635/20. C.W. acknowledegs support through European Commission Marie Curie Research Training Grant CONSTELLATION (MRTN-CT-2006-035890)

REFERENCES

Bastian N., 2008, MNRAS, 390, 759
Boissier S., Gil de Paz A., Boselli A., Madore B. F., Buat V., Cortese L., Burgarella D., Muñoz-Mateos J. C., Barlow T. A., Forster K., Friedman P. G., Martin D. C., Morrissey P., Neff S. G., Schiminovich D., Seibert M., Small T., Wyder T. K., Bianchi L., Donas J., Heckman T. M., Lee Y.-W., Milliard B., Rich R. M., Szalay A. S., Welsh B. Y., Yi, S. K., 2007, ApJS, 173, 524
Chabrier G., 2003, PASP, 115, 763
Diehl R., Halloin H., Kretschmer K., Lichti G. G., Schönfelder V., Strong A. W., von Kienlin A., Wang W., Jean P., Knödlseder J., Roques J.-P., Weidenspointner G., Schanne S., Hartmann D. H., Winkler C., Wunderer C., 2006, Nat, 439, 45
Elmegreen B. G., Scalo J., 2006, ApJ, 636, 149
Figer D. F., 2005, Nat, 434, 192
Fioc M., Rocca-Volmerange B., 1997, A&A, 326, 950
Fioc M., Rocca-Volmerange B., 1999, ArXiv Astrophysics e-prints, arXiv:astro-ph/9912179
Gizis J. E., Reid I. N., Hawley S. L., 2002, AJ, 123, 3356
Hoversten E. A., Glazebrook K., 2008, ApJ, 675, 163
Kennicutt Jr. R. C., 1983, ApJ, 272, 54
Kennicutt Jr. R. C., 1998, ARAA, 36, 189
Kennicutt Jr. R. C., Tamblyn P., Congdon C. E., 1994, ApJ, 435, 22
Koen C., 2006, MNRAS, 365, 590
Köppen J., Weidner C., Kroupa P., 2007, MNRAS, 375, 673
Kroupa P., 2001, MNRAS, 322, 231
Kroupa P., 2002, Sci, 295, 82
Kroupa P., Tout C. A., Gilmore G., 1993, MNRAS, 262, 545
Kroupa P., Weidner C., 2003, ApJ, 598, 1076
Lada C. J., Lada E. A., 2003, ARAA, 41, 57
Lee H.-c., Gibson B. K., Flynn C., Kawata D., Beasley M. A., 2004, MNRAS, 353, 113
Maíz Apellániz J., Walborn N. R., Morrell N. I., Niemela V. S., Nelan E. P., 2007, ApJ, 660, 1480
McKee C. F., Williams J. P., 1997, ApJ, 476, 144
Oey M. S., Clarke C. J., 2005, ApJL, 620, L43
Oke J. B., 1974, ApJS, 27, 21
Oke J. B., 1990, AJ, 99, 1621
Oke J. B., Gunn J. E., 1983, ApJ, 266, 713
Portinari L., Sommer-Larsen J., Tantalo R., 2004, MNRAS, 347, 691
Pflamm-Altenburg J., Kroupa P., 2008, Nat, 455, 641
Pflamm-Altenburg J., Weidner C., Kroupa P., 2007, ApJ, 671, 1550
Recchi S., Calura F., Kroupa P., Matteucci F., 2009, submitted
Reid I. N., Gizis J. E., Hawley S. L., 2002, AJ, 124, 2721xs
Romano D., Chiappini C., Matteucci F., Tosi M., 2005, A&A, 430, 491
Salim S., Rich R. M., Charlot S., Brinchmann J., Johnson B. D., Schiminovich D., Seibert M., Mallery R., Heckman T. M., Forster K., Friedman P. G., Martin D. C., Morrissey P., Neff S. G., Small T., Wyder T. K., Bianchi L., Donas J., Lee Y.-W., Madore B. F., Milliard B., Szalay A. S., Welsh B. Y., Yi S. K., 2007, ApJS, 173, 267
Scalo J. M., 1986, Fundamentals of Cosmic Physics, 11, 1
Tremonti C. A., Heckman T. M., Kauffmann G., Brinchmann J., Charlot S., White S. D. M., Seibert M., Peng E. W., Schlegel D. J., Uomoto A., Fukugita M., Brinkmann J., 2004, ApJ, 613, 898
Tutukov A. V., 1978, A&A, 70, 57
Úbeda L., Maíz-Apellániz J., MacKenty J. W., 2007, AJ, 133, 932
Vanbeveren D., 1983, A&A, 124, 71
Weidner C., Kroupa P., 2004, MNRAS, 348, 187
Weidner C., Kroupa P., 2005, ApJ, 625, 754
Weidner C., Kroupa P., 2006, MNRAS, 365, 1333
Weidner C., Kroupa P., Larsen S. S., 2004, MNRAS, 350, 1503
Wilkins S. M., Hopkins A. M., Trentham N., Tojeiro R., 2008, MNRAS, 391, 363